International Journal of Nanomedicine

Dovepress
open access to scientific and medical research

Open Access Full Text Article

ORIGINAL RESEARCH

Ginseng-berry-mediated gold and silver nanoparticle synthesis and evaluation of their in vitro antioxidant, antimicrobial, and cytotoxicity effects on human dermal fibroblast and murine melanoma skin cell lines

This article was published in the following Dove Press journal:
International Journal of Nanomedicine
17 February 2017
Number of times this article has been viewed

Zuly Elizabeth Jiménez Pérez[1]
Ramya Mathiyalagan[1]
Josua Markus[1]
Yeon-Ju Kim[2]
Hyun Mi Kang[3]
Ragavendran Abbai[1]
Kwang Hoon Seo[2]
Dandan Wang[2]
Veronika Soshnikova[2]
Deok Chun Yang[1,2]

[1]Department of Biotechnology and Ginseng Bank, [2]Department of Oriental Medicine Biotechnology, College of Life Sciences, Kyung Hee University, Yongin, Republic of Korea; [3]Advanced Cosmeceutical Technology R&D Center, Suwon, Republic of Korea

Correspondence: Yeon-Ju Kim; Deok Chun Yang
Department of Oriental Medicine Biotechnology and Ginseng Bank, College of Life Sciences, Kyung Hee University, 1732, Deogyeong-daero, Giheung-gu, Yongin-si, Gyeonggi-do 17104, Republic of Korea
Tel +82 31 201 2100
Fax +82 31 205 2688
Email dcyang@khu.ac.kr; yeonjukim@khu.ac.kr

Abstract: There has been a growing interest in the design of environmentally affable and biocompatible nanoparticles among scientists to find novel and safe biomaterials. *Panax ginseng* Meyer berries have unique phytochemical profile and exhibit beneficial pharmacological activities such as antihyperglycemic, antiobesity, antiaging, and antioxidant properties. A comprehensive study of the biologically active compounds in ginseng berry extract (GBE) and the ability of ginseng berry (GB) as novel material for the biosynthesis of gold nanoparticles (GBAuNPs) and silver nanoparticles (GBAgNPs) was conducted. In addition, the effects of GBAuNPs and GBAgNPs on skin cell lines for further potential biological applications are highlighted. GBAuNPs and GBAgNPs were synthesized using aqueous GBE as a reducing and capping agent. The synthesized nanoparticles were characterized for their size, morphology, and crystallinity. The nanoparticles were evaluated for antioxidant, anti-tyrosinase, antibacterial, and cytotoxicity activities and for morphological changes in human dermal fibroblast and murine melanoma skin cell lines. The phytochemicals contained in GBE effectively reduced and capped gold and silver ions to form GBAuNPs and GBAgNPs. The optimal synthesis conditions (ie, temperature and v/v % of GBE) and kinetics were investigated. Polysaccharides and phenolic compounds present in GBE were suggested to be responsible for stabilization and functionalization of nanoparticles. GBAuNPs and GBAgNPs showed increased scavenging activity against 2,2-diphenyl-1-picrylhydrazyl free radicals compared to GBE. GBAuNPs and GBAgNPs effectively inhibited mushroom tyrosinase, while GBAgNPs showed antibacterial activity against *Escherichia coli* and *Staphylococcus aureus*. In addition, GBAuNPs were nontoxic to human dermal fibroblast and murine melanoma cell lines, and GBAgNPs showed cytotoxic effect on murine melanoma cell lines. The current results evidently suggest that GBAgNPs can act as potential agents for antioxidant, anti-tyrosinase, and antibacterial activities. In addition, GBAuNPs can be further developed into mediators in drug delivery and as antioxidant, anti-tyrosinase, and protective skin agents in cosmetic products. Consequently, the study showed the advantages of using nanotechnology and green chemistry to enhance the natural properties of GBs.

Keywords: ginseng berry, nanoparticles, antibacterial, antioxidant, anti-tyrosinase, cytotoxicity

Introduction

The accelerated expansion of the studies in nanotechnology has resulted in an extensive set of nanoparticles that differ in size, shape, charge, capping layer, and stability.

submit your manuscript | www.dovepress.com
Dovepress
http://dx.doi.org/10.2147/IJN.S118373

However, the major challenge for scientists is the creation of novel nanoparticles without the use of toxic chemicals to eliminate the risks in cosmetic, pharmaceutical, and biomedical applications. Hence, harmless solvents, nontoxic reducing agents, and renewable materials are key in the production of environmentally affable and biocompatible nanoparticles.

Accordingly, green synthesis meets the requirements of nontoxic nanoparticles.[1] Moreover, it increases the utilization value of the particular organisms. In particular, plant or fruit extracts are more beneficial than fungal- or microbial-mediated syntheses since they eliminate the time-consuming process of maintaining cells and avoid high cost that can be suitably restrained for extensive productions under non-aseptic environments. In this study, we highlight the utilization of ginseng berries (GBs) as both reducing and stabilizing agents to form multifunctional gold nanoparticles (AuNPs) and silver nanoparticles (AgNPs) by green chemistry.

Panax ginseng Meyer is a medicinal plant that belongs to Araliaceae family.[2] It has penetrated the global market as health food and has been implemented as an active ingredient in herbal cosmetics. The major active components of *P. ginseng* are ginsenosides, a diverse group of steroidal saponins, which boast the ability to target a large number of tissues and produce a cluster of pharmacologic responses. Pharmacological effects of ginseng include anticancer, antistress, antifatigue, and antioxidant activities and aging-inhibitory effects.[3] Ginseng also has other bioactive ingredients such as phenolic compounds, acid polysaccharides, and essential proteins.[4] These bioactive compounds are not evenly distributed along the structure of ginseng plant. Particularly, the content of bioactive compounds differs between ginseng roots, leaves, and berries.[5] Phytochemical profile of GB is significantly different compared to ginseng root; it has been reported that ginsenoside Re is notably higher in GB than in the ginseng root.[6] In addition, GB extracts (GBEs) are also a rich source of vitamin E, vitamin K, folic acid, and potassium.[7] GB has been reported to possess antioxidation, anti-inflammation, collagen synthesis facilitation, skin wrinkle care, whitening, moisturizing, skin barrier improvement, and atopy alleviation effects.[8] The growing studies of GBs seem to point to their health benefits in skin treatments. Among all the biological effects of GBE on skin, protective effects against photoaging and collagen synthesis are of remarkable importance. Collagen represents the main component of the extracellular matrix of dermal connective tissue. The matrix metalloproteinases (MMPs) play an important role in the reduction of collagen in the extracellular matrix of connective tissues. Interstitial collagenase (MMP-1) degrades the collagens, types I, II, and III.[9] Yeom et al[10] reported that GBE had antioxidant effect against oxidative stress and inhibited the expression of MMP-1 in ultraviolet (UV)-irradiated human dermal fibroblast (HDF) cell lines; the study also confirmed that GBE's main compound ginsenoside Re increased hyaluronic acid in HaCaT keratinocytes. A study by Jeon et al[11] reported that GBE antioxidant activity is responsible for the increase of procollagen type I gene expression, the decrease of MMP-1 gene expression, and the suppression of tumor necrosis factor gene expression in HDF cells. The same author has reported that GBE efficacy increases after fermentation with lactic acid bacteria. Recently, Kim et al[12] reported that the antimelanogenic activity of GB was related to the activation of the longevity gene *foxo3a* in human melanoma MNT1. In addition, the antiaging effects of GB caused a life span extension and reduced lipofuscin accumulation in *Caenorhabditis elegans* wild-type N2.

This study introduced the green synthesis of AuNPs and AgNPs based on the unique phytochemical profile of GBs. We propose that the synergetic bioreduction mechanisms of ginsenosides, phenolic compounds, acid polysaccharides, and proteins present in the aqueous extract of GBs are able to reduce and stabilize metal salts into nanoparticles, which are then targeted for potential applications in cosmetics. The assessment of this green synthesis will lead to more cost-effective and benign nanoparticles with functional biological applications. The boundless properties of AuNPs and AgNPs encourage their usefulness in a large number of environmental and biomedical applications such as biomedical imaging, drug delivery, cosmetics, wound healing, and antibacterial agents.[13]

Materials and methods

Materials

Gold (III) chloride trihydrate ($HAuCl_4 \cdot 3H_2O$), silver nitrate ($AgNO_3$), and 2,2-diphenyl-1-picrylhydrazyl (DPPH) were purchased from Sigma-Aldrich (St Louis, MO, USA). Arbutin and L-3,4-dihydroxyphenylalanin (L-DOPA) were obtained from Abcam (Cambridge, UK). Dulbecco's Modified Eagle's Medium (DMEM), high glucose, and pyruvate were purchased from Gibco (Waltham, MA, USA). Fetal bovine serum (FBS) and penicillin–streptomycin solution were purchased from GenDEPOT (Barker, TX, USA). Soluble MTT was purchased from Life technologies (Eugene, OR, USA). The standard neomycin (30 µg/disk) antibiotic disks were obtained from Becton, Dickinson, and Company (Seoul, South Korea). The strains *Staphylococcus aureus* (ATCC6538) and *Escherichia coli* (BL-21) were used for antimicrobial studies. The bacterial strains were cultured on nutrient agar media at 37°C and preserved at −70°C in glycerol stock vials for further study.

Phytochemical analysis of GB

Analysis of the content of ginsenosides

Fresh *P. ginseng* Meyer berries were collected from 4-year-old *P. ginseng* plants from Gochang, Republic of Korea. The berries were subsequently dried and ground into fine powder. GB was subjected to high-performance liquid chromatography (HPLC) analysis according to a previously described method with slight modifications.[4] Briefly, 1 g of the dried GB powder was extracted three times with 20 mL of 80% CH_3OH–H_2O at 80°C for 2 h. The solvent was evaporated at 40°C in a rotary evaporator. The extract was then dissolved in 1 mL of CH_3OH, filtered through a 0.45 µm filter, and then analyzed by HPLC (Agilent 1260, Palo Alto, CA, USA) analysis. Ginsenosides were resolved on a C_{18} column (50 mm × 3.0 mm, inner diameter 2.7 µm) with H_2O (solvent A) and acetonitrile (solvent B) at A:B ratios of 83:17, 83:17, 71:29, 60:40, 30:70, 10:90, 10:90, 83:17, and 83:17, with run times of 0, 6, 9, 14, 17, 18.5, 22, 22.5, and 26 min, respectively. The flow rate was 1.0 mL/min, and the detection wavelength was 203 nm.

Analysis of reducing sugars

The content of reducing sugars in GBE was estimated using dinitrosalicylic acid (DNS) reagent method as described in a previous report.[4] GB CH_3OH–H_2O extract (1 mL) and DNS reagent (1 mL) were boiled in oil bath for 5 min and cooled to room temperature. Sample absorbance of the reaction mixture was measured at 550 nm by UV–visible (vis) spectrophotometer. The content of reducing sugars was calculated from a calibration curve using glucose as a reference.

Analysis of total phenolic content

The Folin–Ciocalteu method was followed for the determination of total phenolic content of GB. Reaction mixture containing GB CH_3OH–H_2O extract (1 mL) and 10% Na_2CO_3 (1 mL) was incubated at room temperature for 3 min. Approximately 1 mL of Folin–Ciocalteu reagent (2 N) was added. The solution was kept in dark for 30 min, and then absorbance was measured at 750 nm. The content of total phenolic was calculated from calibration curves using gallic acid as a reference.

Analysis of acidic polysaccharides

One gram of dried GB powder was extracted in distilled water (DW) at 80°C for 1 h. Next, ethanol was added to the extraction, and the reaction mixture was shaken for 4 h to isolate polysaccharides. The solution was centrifuged, and the supernatant was removed, evaporated in a rotary evaporator at 40°C, and diluted in DW to make 1 mg/mL of the sample. Acidic polysaccharides were measured using *m*-hydroxydiphenyl method with slight modifications.[14] Approximately 0.2 mL of the sample was mixed with 1.2 mL of $Na_2B_4O_7{\cdot}10H_2$–H_2SO_4 (12.5 mM), boiled in water bath at 100°C for 5 min, and cooled in ice bath. Then, 20 µL of *m*-hydroxydiphenyl reagent was added to the sample. The sample was shaken, and its absorbance was read at 520 nm by UV–vis spectrophotometer within 5 min.

Preparation of aqueous extract of *P. ginseng* Meyer berry

Approximately 10 g of GB powder was dissolved in 150 mL of sterile DW. The solution was autoclaved at 100°C for 30 min. The slurry was filtered using Whatman filter paper. The total filtrate of GBE was stored at −20°C for further use in nanoparticle synthesis.

Green synthesis of AuNPs and AgNPs

AuNPs and AgNPs were synthesized as reported earlier with some modifications.[15] Gold (III) chloride trihydrate ($HAuCl_3{\cdot}3H_2O$) and silver nitrate ($AgNO_3$) were used as precursor salts for the synthesis of AuNPs and AgNPs, respectively. 1) Nanoparticles were synthesized by adding gold and silver salts into 100 mL of GBE to reach a final concentration of 1 mM. 2) To study the effects of temperature, AuNPs and AgNPs were synthesized at different temperatures (23°C, 40°C, 60°C, 80°C, and 90°C). The progress of the reaction was monitored by measuring the absorbance of the solution at regular time intervals. Finally, a color change in the solution indicated the formation of AuNPs and AgNPs in the respective reaction mixtures. After color change was observed, AuNPs and AgNPs were purified by physical methods. The reaction mixture was centrifuged at 10,000 rpm for 20 min to remove undesirable components. Then, biosynthesized nanoparticles were purified by continuous washing with sterile DW and centrifugation at 16,000 rpm for 15 min to obtain nanoparticles in pellet form. Finally, the purified nanoparticles were air dried overnight and obtained in powder form. Kinetics of the bioreduction was studied by recording UV–vis absorbance at the optimal temperature as a function of time.

Characterization of AuNPs from GB (GBAuNPs) and AgNPs from GB (GBAgNPs)

The purified nanoparticles were characterized by UV–vis spectrophotometer, field-emission transmission electron microscopy (FE-TEM), energy-dispersive X-ray spectrometer (EDX), X-ray diffraction (XRD), selected area electron

diffraction (SAED), elemental mapping, particle size analyzer, and Fourier transform infrared (FTIR) spectrometer.

UV–vis spectra of synthesized nanoparticles were measured in the range of 300–800 nm by UV–vis spectrophotometer. FE-TEM, EDX, SAED, and elemental mapping of nanoparticles were obtained by JEM-2100F electron microscope operated at a voltage of 200 kV. Droplets of purified nanoparticles were placed on carbon-coated copper grids and allowed to dry in an oven at 60°C.

The characterization of the crystal structure of the nanoparticles was analyzed by X-ray diffractometer (Bruker, Rheinstetten, Germany). X-ray diffractometer was operated at 40 kV, 40 mA, with CuKα radiation of 1.54 Å, scanning rate of 6°/min, and a step size of 0.02°. Samples were scanned over the 2θ range of 20°–80°. The average crystal size diameter of metal nanoparticles was calculated by Debye–Scherrer equation: $D = 0.9\lambda/\beta \cos\theta$, where D is the crystallite size in nm, λ is the wavelength of CuKα radiation in nm, β is the full width at half maximum (FWHM) in radians, and θ is the half of the Bragg angle in radians.

The particle size distribution of the nanoparticles suspended in DW was obtained by dynamic light scattering (DLS; Otsuka Electronics, Shiga, Japan). The hydrodynamic (Z-average) diameter and polydispersity index (PDI) were evaluated at 25°C. A dispersive medium of pure water with a refractive index of 1.3328, viscosity of 0.8878, and dielectric constant of 78.3 was used as a reference. FTIR measurements of nanoparticles were performed on a PerkinElmer Spectrum One FTIR spectrometer in the range of 4,000–450 cm^{-1} and at a resolution of 4 cm^{-1}.

In vitro stability studies of GBAuNPs and GBAgNPs

In vitro stability of the GBAuNPs and GBAgNPs was tested in the presence of DW, 20 mM of glycine–HCl buffer (pH 2.0), citric acid–sodium citrate buffer (pH 5.0), sodium phosphate buffer (pH 7.0), Tris–HCl buffer (pH 8.0), 5% NaCl, 10% NaCl, and 5% bovine serum albumin (BSA) solutions. Approximately 100 µL of metal nanoparticle solution was added to 900 µL of the mentioned solvents and incubated at 37°C. The stability of nanoparticles was confirmed if there was no significant alteration in surface plasmon wavelength by UV–vis spectrophotometer.

In vitro biological activity of GBAuNPs and GBAgNPs

Free radical scavenging activity of GBAuNPs and GBAgNPs

The potential antioxidant activity of GBAuNPs, GBAgNPs, and GBE was determined based on free radical scavenging activity of the stable 2,2-diphenyl-1-picrylhydrazyl (DPPH). Aliquots of 160 µL of 0.1 mM methanolic solution of DPPH were added to 40 µL of nanoparticle solution containing different concentrations (2–20 µg/mL) of GBAuNPs and GBAgNPs. Gallic acid was used as a positive control. Absorbance values at 517 nm were determined after 30 min by UV–vis spectrophotometer. The percent inhibition activity was calculated as follows:

$$\frac{\text{Absorbace of control} - \text{absorbance of sample}}{\text{Absorbance of corntrol}} \times 100$$

where "absorbance of sample" is the absorbance of the DPPH solution with nanoparticles and "absorbance of control" is the absorbance of the DPPH solution without nanoparticles.[16] Half maximal inhibitory concentration (IC_{50}) values denoting the concentration of sample required to scavenge 50% DPPH free radicals were calculated graphically.

Effect of GBAuNPs and GBAgNPs on mushroom tyrosinase activity

The activity of mushroom tyrosinase was spectrophotometrically determined as described earlier with minor modifications.[17] L-DOPA (2 mM, 0.05 mL) in phosphate-buffered saline (PBS; 50 mM, pH 6.8) and 0.05 mL of the same buffer with or without test sample were added to a 96-well microplate, and then 0.05 mL of mushroom tyrosinase (200 U/mL) was mixed. After incubating the mixture at 37°C for 30 min, the optical density was measured at 490 nm by Synergy 2 Multi-Mode Reader (Bio-Tek Instruments, Inc., Vinooski, VT, USA). The inhibition rate of tyrosinase was calculated as follows: $\% = [(A - B)/A] \times 100$, where A indicates the difference of absorbance without the sample and B indicates the absorbance with enzyme or sample. In this study, arbutin (25 and 100 µg/mL) was used as a standard.

Antimicrobial activity of GBAgNPs against *E. coli* and *S. aureus*

The antimicrobial activity of nanoparticles was studied against *E. coli*, and *S. aureus* on Mueller-Hinton agar (MHA) plates using the disk diffusion method as previously reported.[18] In this assay, the MHA plates were spread evenly with 100 µL of an overnight log culture of test organisms in lysogeny broth (LB) with an optical density of 0.1. Standard antibiotic disk of neomycin was maintained as control. Next, sterile paper disks were further impregnated by different concentrations of freshly prepared and purified AgNP and AuNP solution (15, 30, and 45 µg/disk). The plates were incubated at 37°C for 24 h. After the incubation period, the zones of inhibition around each disk were compared according to the previous method.

Cell viability assay of GBAuNPs and GBAgNPs in HDF and murine melanoma B16BL6 (B16) cell lines

HDF and B16 cell lines were obtained from the Korean Cell Line Bank (Seoul, Korea). Cell lines were cultured in DMEM supplemented with 10% FBS and 1% penicillin–streptomycin at 37°C in a humidified 95% air/5% CO_2 atmosphere as described earlier.[19,20] The cytotoxic effect of nanoparticles on cell viability was measured by MTT assay method. Cells were seeded at a density of 1×10^5 in 96-well plate and cultured for 24 h. At 90% confluence, cells were treated with various concentrations of GBAuNPs or GBAgNPs (0.1–100 µg/mL) for 72 h. After 3 days of incubation, 10 µL of MTT assay solution (5 mg/mL in PBS) was added to each well and further incubated at 37°C for 3 h. Finally, 100 µL of dimethyl sulfoxide was added to dissolve the formazan crystals. The absorbance was measured at 570 nm with a reference wavelength of 630 nm by an ELISA reader.

Statistical analysis

All data are presented as mean ± standard error. All experiments were independently performed for three times. The mean values of the treatment groups were compared with untreated groups using Student's *t*-test. Statistical significance was assigned at $*P<0.05$.

Results and discussion

The aim of this study was to design and develop biocompatible AuNPs and AgNPs for subsequent use in medical applications and to prove the direct intervention of phytochemicals in GBE for the production of novel and functional nanoparticles. To our knowledge, this is the first report on the biosynthesis of AuNPs and AgNPs by GBE without the addition of hazardous solvents and capping agents. The biosynthesis of AuNPs and AgNPs employs the direct interaction of gold and silver salts conjointly with GBE. DW was utilized as solvent, and aqueous extract from berries of *P. ginseng* Meyer was selected as the reducing and stabilizing agent. Consequently, this reaction pathway satisfies all the conditions of a 100% green chemical process.[21]

Phytochemical analysis of GB

Specific details on the nature and chemical roles of different phytochemicals found in GB responsible for the production of GBAuNPs and GBAgNPs are summarized in the following sections. The main phytochemicals present in GB are ginsenosides, acidic polysaccharides, polyphenols, and reducing sugars.[22] The ginsenoside content of GBs was analyzed by HPLC and is shown in Figure 1. The HPLC profile of GBE showed that ginsenosides Re, Rd, Rg_2, Rh_2, and Rb_2 were found to be the predominant saponins.

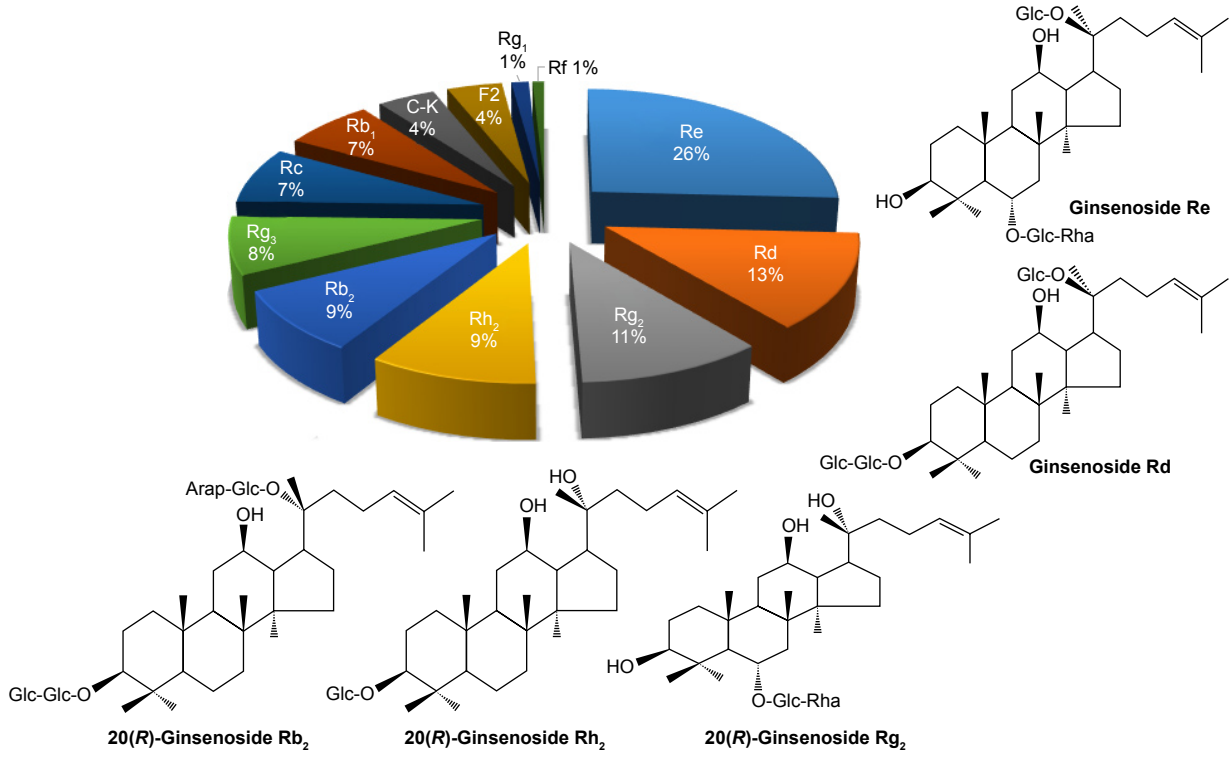

Figure 1 Composition of ginsenosides in GBE.
Abbreviation: GBE, ginseng berry extract.

Ginsenoside Re was found to be the most abundant ginsenoside in the berries. This result is in accordance to the previous study.[22] One of the advantages is that GBE rich in ginsenoside Re promoted hyaluronic acid content in HaCaT cell lines.[10] This study revealed that GBE is a rich source of polyphenols (403.3±0.03 μg/g), which promote the natural protection of skin against UV damage and antioxidant activity. Reducing sugars (5.02±1.70 mg/g) present in GBE are environmentally friendly and stabilizing agents. Our study confirms that the content of acidic polysaccharides in GBE was 136.7±5.70 μg/mL. Many pharmacological studies have shown that acidic polysaccharides from GBE have favorable biological properties, such as collagen production, antioxidant, immunomodulation, and radioprotective effects.[23,24]

The various compositions of phytochemicals in GBE (Figure 2) provide functionalization and stabilization further onto the nanoparticle matrix. In addition, phytochemicals present in GBE are presumably responsible for the creation of a robust coating on AuNPs and AgNPs, thus rendering the nanoparticles stable against agglomeration.

Effect of temperature, kinetics, and GBE concentration of GBAuNP and GBAgNP synthesis by UV–vis spectroscopy

Reaction temperature and GBE concentration were optimized for the large-scale bioreduction of $HAuCl_4$–$3H_2O$ and $AgNO_3$. The formation of AuNPs and AgNPs was confirmed by using UV–vis spectral analysis at different reaction temperatures, times, and GBE concentrations. The formation of nanoparticles was controlled by varying temperature of synthesis and keeping the concentration of gold and silver salts (1 mM) and GBE (3% v/v) constant. Figure 3A and B illustrates the effect of temperature on the formation of GBAuNPs and GBAgNPs. It is observed that at ambient temperature (23°C), surface plasmon wavelengths of AuNPs and AgNPs could be observed at 540 and 444 nm, respectively, albeit with a slow reduction rate; total reaction times of AuNPs and AgNPs were completed in 270 min and 24 h, respectively. When reaction temperature was raised to 90°C, major absorption peaks at 530 and 422 nm of both GBAuNPs and GBAgNPs became more significant. Increasing the reaction temperature greatly decreases the reaction times and leads to a decrease in nanoparticle size; the largest absorption peaks of AuNPs and AgNPs at 90°C were observed in 25 min and 3 h, respectively. In addition to faster reaction times, shifts in surface plasmon wavelengths were also evident, meaning that at higher temperature (90°C), AuNPs and AgNPs became smaller in size.[25] The wavelengths that registered at lower temperatures (23°C–60°C) indicated larger particle size in both nanoparticles. Moreover, the rate of gold reduction was much faster compared to that of silver ions. This is due to the fact that standard reduction potential of Au^{3+}/Au is higher than Ag^{+}/Ag.[26] Furthermore, no detectible change in the peak intensity and the same intensity of ruby red color were observed after 25 min of incubation, suggesting a nano-sized distribution of AuNPs and completion of the bioreduction.

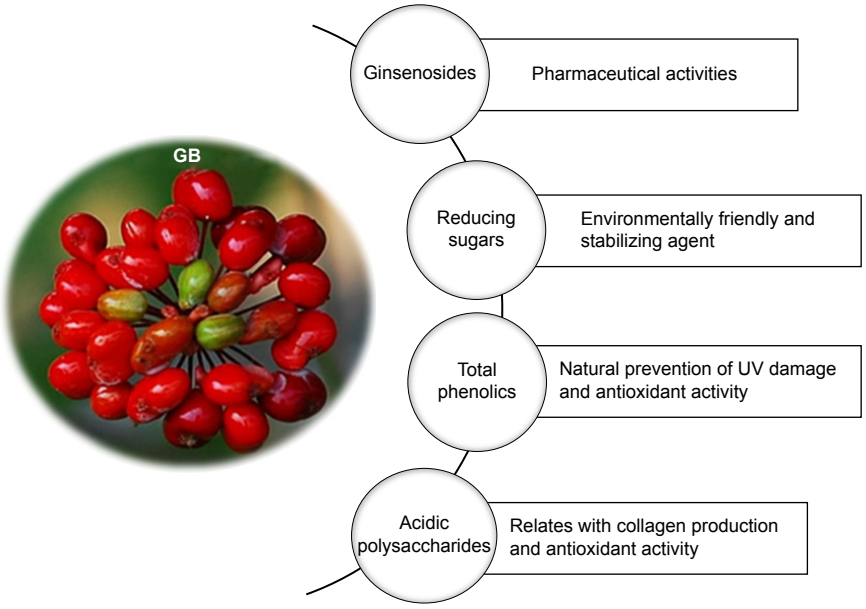

Figure 2 Phytochemical properties of *Panax ginseng* berry.
Abbreviations: GB, ginseng berry; UV, ultraviolet.

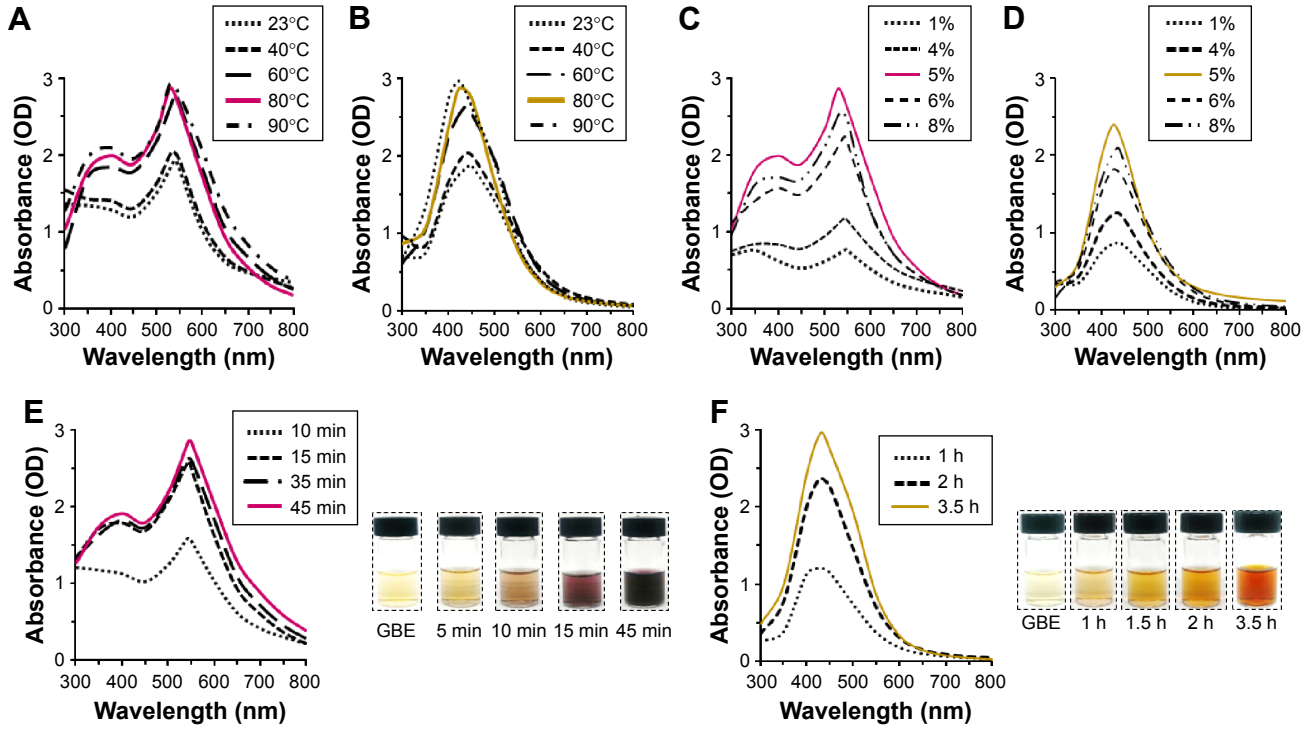

Figure 3 Reaction temperature and concentration of GBE have been successfully optimized to maximize the yield of nanoparticles.
Notes: Temperature-dependent evolution of UV–vis spectra of synthesized nanoparticles at a constant amount of GBE (3%, v/v) and 1 mM of gold and silver salts: (**A**) GBAuNPs and (**B**) GBAgNPs. Concentration-dependent evolution of UV–vis at 80°C of (**C**) GBAuNPs (**D**) GBAgNPs. Time-dependent evolution of UV–vis at 80°C, GBE 5% concentration of GBE and the respective photograph which shows the color change pattern during nanoparticle synthesis of (**E**) GBAuNPs and (**F**) GBAgNPs.
Abbreviations: GBAgNPs, silver nanoparticles from ginseng berry; GBAuNPs, gold nanoparticles from ginseng berry; GBE, ginseng berry extract; OD, optical density; UV, ultraviolet; vis, visible.

Different concentrations of GBE (1%–8%, v/v) were adopted to find the optimal concentration of the extract. Concentrations of gold and silver salts (1 mM) and optimal reaction temperature (80°C) were kept constant. Results showed that optimal concentration of GBE was 5% (Figure 3C and D). The intensity of peak is directly proportional to the concentration of nanoparticles in the solution.[27] However, an increase in the wavelength of GBAuNPs from 530 to 544 nm was observed with further increase in the GBE (6%, v/v). Similar variation in wavelength from 426 to 434 nm was also observed in UV–vis spectra of GBAgNPs when the concentration of GBE was increased to 6% (v/v). Both results suggest the probability of increased particle sizes. Higher concentrations of fruit extract introduce more reducing and stabilizing agents into the reaction mixture, which result in a secondary reduction process on the surface of preformed nuclei and additional interactions between surface biomolecules, resulting in larger particles. The reduction in gold and silver salts was visually observed from the color change of the reaction mixture. Reaction mixtures turned to purple and brown within 45 min and 3.5 h of incubation at 80°C, respectively. The intense color change is the response of surface plasmon resonance due to the oscillation of free electrons in the conduction band of metal nanoparticles (Figure 3E and F).[28] Finally, activation energy, E_a, and rate constants, k, were calculated from Arrhenius equation to determine the optimal reaction temperature. The values of rate constants at different temperatures are shown in Table 1. As the reaction temperature is increased to 80°C, the rate constants became larger (ie, reduction becomes kinetically more agreeable). However, the rate constant at 90°C is less than the rate constant measured at 80°C. This may be caused due to metal

Table 1 Rate constants at different temperatures

Temperature (°C)	24		40		80		90	
	GBAgNPs	GBAuNPs	GBAgNPs	GBAuNPs	GBAgNPs	GBAuNPs	GBAgNPs	GBAuNPs
k (min^{-1})[a]	1.10×10^{-3}	2.26×10^{-2}	3.30×10^{-3}	4.05×10^{-2}	1.82×10^{-2}	3.20×10^{-1}	1.72×10^{-2}	1.97×10^{-1}

Note: [a]Values are mean ± SD of triplicate measurements.
Abbreviations: GBAgNPs, silver nanoparticles from ginseng berry; GBAuNPs, gold nanoparticles from ginseng berry; SD, standard deviation.

nanoparticle aggregation at higher temperature due to more frequent collisions.[29] Furthermore, the activation energies of gold and silver bioreduction were calculated to be 33.60 and 37.32 kJ/mol, respectively. The bioreduction of silver has a higher E_a value, and thus the reaction is more sensitive to temperature change than the bioreduction of gold.

Structural and morphological characterization of GBAuNPs and GBAgNPs and their particle size distributions

Structural properties, such as size and morphology, of AuNPs and AgNPs were determined by two independent techniques, such as FE-TEM and DLS. FE-TEM was used to determine the metallic core size of metal nanoparticles, while DLS was used to evaluate the hydrodynamic size (Z-average) of GB-coated AuNPs and AgNPs. FE-TEM measurements of GBAuNPs and GBAgNPs showed that the particles are spherical in shape with sizes varying from 5 to 10 and 10 to 20 nm, respectively. Size distribution analysis of GBAuNPs and GBAgNPs confirmed that nanoparticles are polydispersed (Figure 4A and B). DLS method was employed to calculate the hydrodynamic radii of nanoparticles coated with phytochemicals. The GBE phytochemical coatings on AuNPs caused substantial changes in the hydrodynamic radii of GBAuNPs and GBAgNPs. The hydrodynamic diameters of GBAuNPs and GBAgNPs as determined from DLS measurements gave values of 179 nm with PDI of 0.26 and 580 nm with PDI of 0.25, respectively, suggesting that much of the GBE phytochemicals (ginsenosides, acidic polysaccharides, polyphenols, and reducing sugars) were capped onto AuNPs and AgNPs.

EDX and elemental mapping analysis of GBAuNPs and GBAgNPs

The EDX analysis confirmed the presence of characteristic peaks of metallic gold and silver at 2.2 and 3.3 keV, respectively (Figure 4C and D).[30] EDX profile shows a strong gold or silver signal in the synthesized nanoparticles, while elemental mapping analysis of the purified GBAuNPs and GBAgNPs showed the maximum distribution of the gold and silver elements in the corresponding nanoparticles (Figure 4E and F). The resulting distribution patterns of the GBAuNPs and GBAgNPs were similar to the distribution patterns of AuNPs and AgNPs synthesized by using red ginseng root extract.[31]

XRD and SAED analysis of GBAuNPs and GBAgNPs

The XRD spectra were recorded for the identification of crystallinity exhibited by the synthesized materials. The synthesized GBAuNPs showed four major diffraction

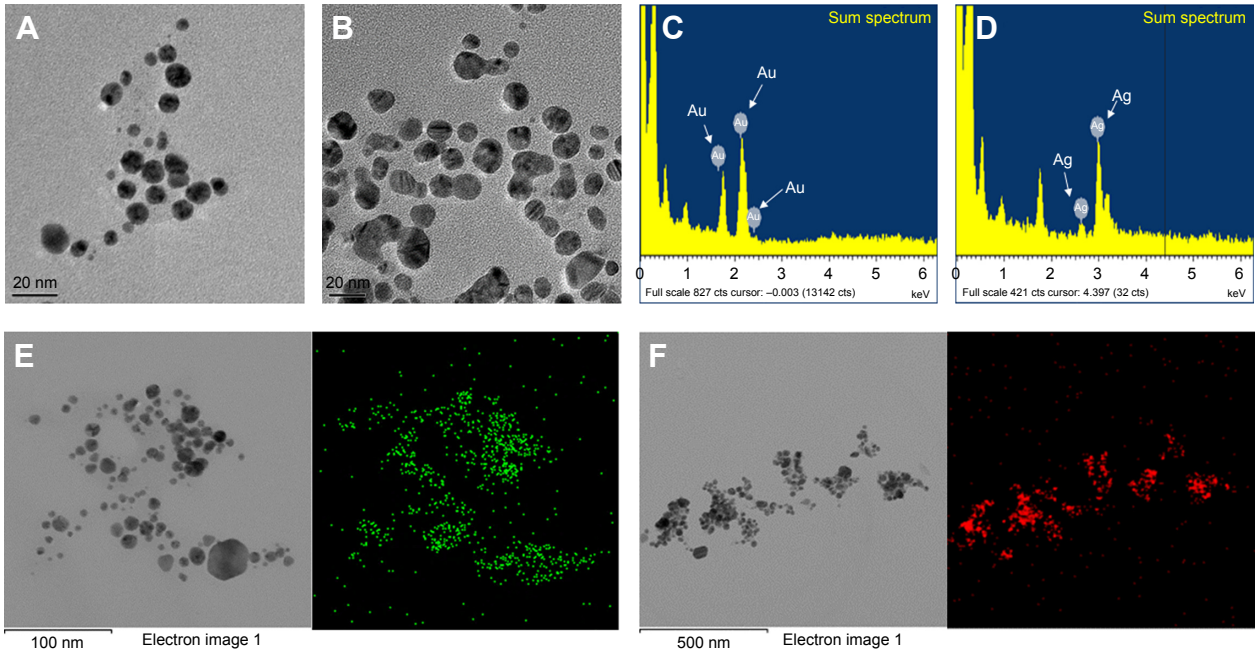

Figure 4 FE-TEM imaging shows that the particles are spherical in shape.

Notes: (**A**) GBAuNPs with sizes between 5 and 10 nm and (**B**) GBAgNPs with sizes between 10 and 20 nm. EDX spectrum of (**C**) GBAuNPs confirmed the presence of characteristic peak of metallic gold at 2.2 keV and (**D**) GBAgNPs characteristic peak of silver at 3.3 keV. Elemental mapping analysis of (**E**) GBAuNPs and (**F**) GBAuNPs showed maximum distribution of gold (green) and silver (red) elements in the corresponding nanoparticles.

Abbreviations: EDX, energy-dispersive X-ray spectrometer; FE-TEM, field-emission transmission electron microscopy; GBAgNPs, silver nanoparticles from ginseng berry; GBAuNPs, gold nanoparticles from ginseng berry.

peaks at 2θ values of 38.48°, 44.60°, 65.25°, and 78.21° which correspond to (111), (200), (220), and (311) planes, respectively (Figure 5A).

The synthesized GBAgNPs showed four diffraction peaks at 2θ values of 38.37°, 45.85°, 63.98°, and 77.90° which correspond to (111), (200), (220), and (311) planes, respectively (Figure 5B). The average crystallite sizes of GBAuNPs and GBAgNPs were found to be 4.24 and 1.69 nm, respectively. SAED pattern of GBAuNPs (Figure 5C) and GBAgNPs (Figure 5D) indicated a face-centered cubic crystal structure.[32]

FTIR analysis of GBAuNPs and GBAgNPs

The functionality of GBE and their nanoparticles was analyzed by FTIR analysis. Both FTIR spectra of GBE and the resulting nanoparticles (ie, GBAuNPs and GBAgNPs) are shown in Figure 6; few characteristic peaks were transmitted at the same wavenumbers, indicating that some phytochemicals contained in the extract were present on the surface of the nanoparticles. The characteristic peaks of polysaccharide and hydroxyl group of phenolic compounds structures due to O–H stretching are shown between 3,500 and 3,000 cm^{-1}.[20,26] C–H stretching between 3,000 and 2,800 cm^{-1} was due to C–H stretching vibration of methyl or methylene group.[33,34] The pronounced peaks between 1,600 and 1,400 cm^{-1} represented carbonyl group stretching vibration of flavonoids and ester bonds in polyphenolic compounds.[35] Weak peaks between 1,500 and 1,032 cm^{-1} corresponded to aromatic C–C groups and C–O functional in tanning/tannic acid.[36] A peak between 1,200 and 1,000 cm^{-1}

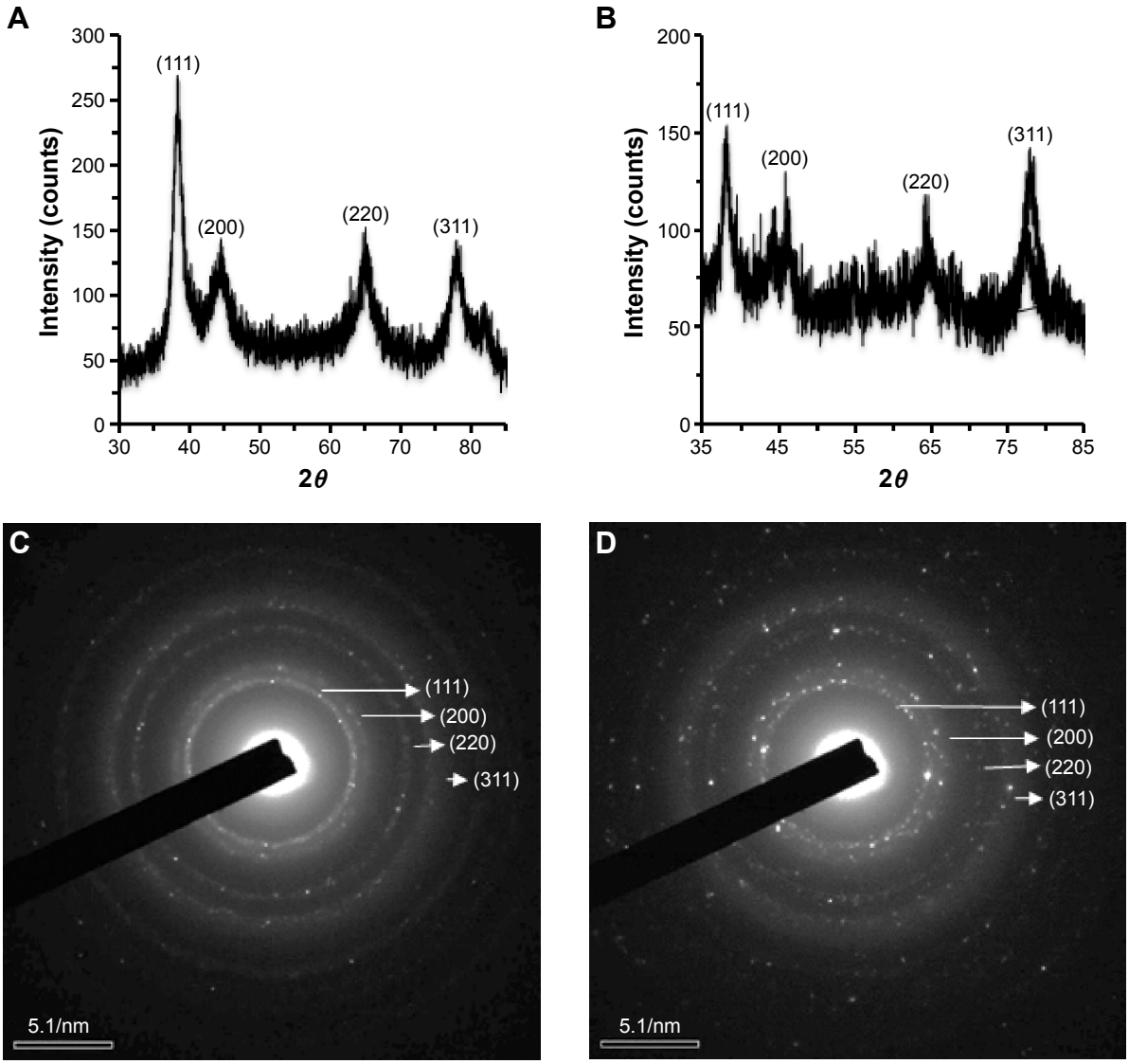

Figure 5 XRD pattern for the identification of crystallinity exhibited by the synthesized materials.
Notes: (**A**) GBAuNPs and (**B**) GBAgNPs. SAED pattern indicated that an FCC crystal structure of (**C**) single GBAuNPs is spherical and (**D**) single GBAgNPs is spherical.
Abbreviations: FCC, face-centered cubic; GBAgNPs, silver nanoparticles from ginseng berry; GBAuNPs, gold nanoparticles from ginseng berry; SAED, selected area electron diffraction; XRD, X-ray diffraction.

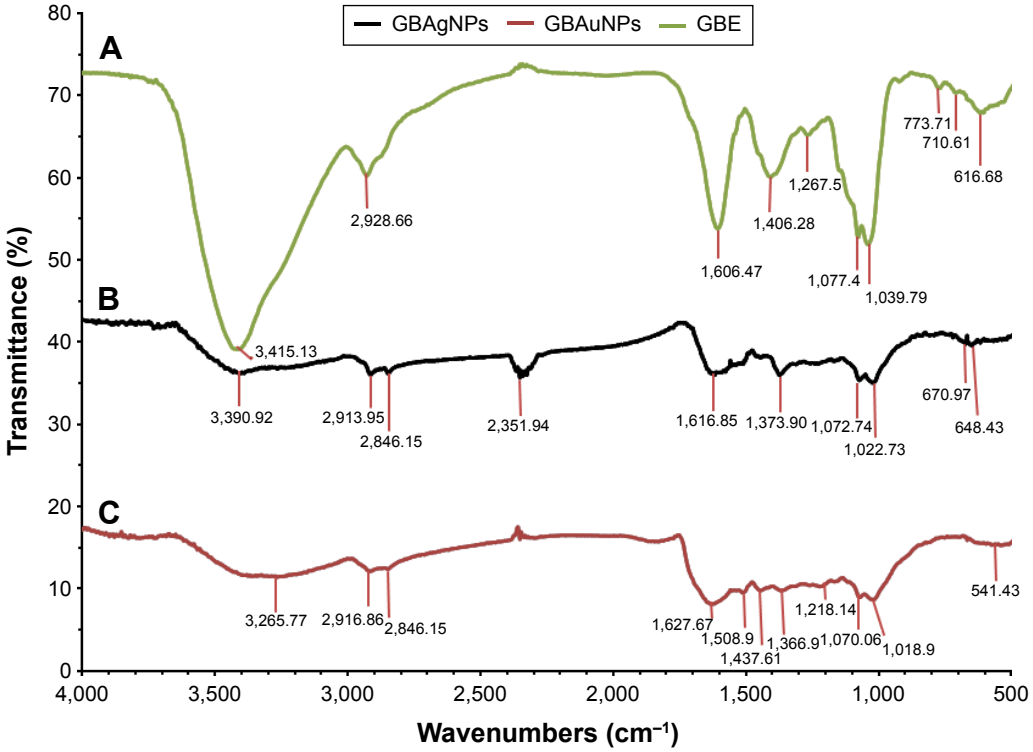

Figure 6 FTIR spectra of (**A**) GBE, (**B**) GBAgNPs and (**C**) GBAuNPs.
Notes: The peaks of polysaccharide and hydroxyl group of phenolic compound structures due to O–H stretching are shown between 3,500 and 3,000 cm^{-1}. C–H stretching between 3,000 and 2,800 cm^{-1} corresponds to methyl and methylene group, and peaks between 1,600 and 1,400 cm^{-1} represent carbonyl group stretching vibration of flavonoids and ester bonds in polyphenolic compounds. Weak peaks between 1,500 and 1,032 cm^{-1} corresponds to aromatic C–C groups and C–O functional in tanning/tannic acid.
Abbreviations: FTIR, Fourier transform infrared; GBAgNPs, silver nanoparticles from ginseng berry; GBAuNPs, gold nanoparticles from ginseng berry; GBE, ginseng berry extract.

was found in association with the C−O−H and C−O−C band positions. Based on the FTIR spectral analysis for the surface adhered biomolecules and experimental work, polysaccharides, flavonoids, tannins, phenolic glycosides, and reducing sugars from GBE may be responsible for the reduction and subsequent stabilization of biosynthesized nanoparticles.

In vitro stability studies of GBAuNPs and GBAgNPs

The stability of GBAuNPs and GBAgNPs was evaluated by monitoring the wavelengths in the presence of DW, 5% NaCl, 10% NaCl, 5% BSA, and different pH conditions (pH 2.0–8.0) at 37°C. The wavelengths in DW, pH 2, pH 7, pH 8, 10% NaCl, and 5% BSA solution for GBAuNPs and GBAgNPs resulted in minimal wavelength shifts (0–5 nm) after 1 day of incubation at 37°C. In the case of GBAuNPs, there was no major shift in wavelength in all prescribed conditions after 1 month. However, GBAgNPs showed long-term stability in DW and 5% BSA after 1 month. Our results confirmed that the GBAuNPs and GBAgNPs are intact and, thus, demonstrated excellent in vitro stability in biological fluids at physiological pH condition.

The current discovery of the unique chemical power of phytochemicals in GBE in initiating nanoparticle formation is of paramount importance in the context of the production of AuNPs and AgNPs for medical and technological applications under nontoxic conditions. One of the paramount prerequisites of utilizing AuNPs for in vivo imaging and therapy applications is that the nanoparticles can be produced and stabilized in biologically benign media.

Antioxidant activity of GBAuNPs and GBAgNPs

The results of our study revealed that the synthesized nanoparticles exhibited free radical scavenging activity (Figure 7A). However, GBAgNPs showed the highest free radical scavenging activity (93.8%) compared to GBAuNPs (81.5%) and GBE (81%). In vitro DPPH radical scavenging assay showed that GBAgNPs (IC_{50} =1.85 µg/mL) had the highest level of antioxidant activity followed by GBE (IC_{50} =1.90 µg/mL and GBAuNPs (IC_{50} =1.96 µg/mL). The possible reason for high antioxidant activity of GBE may be correlated to the presence of copious bioactive compounds present in it. Moreover, the increased antioxidant activity of GBAgNPs can be credited

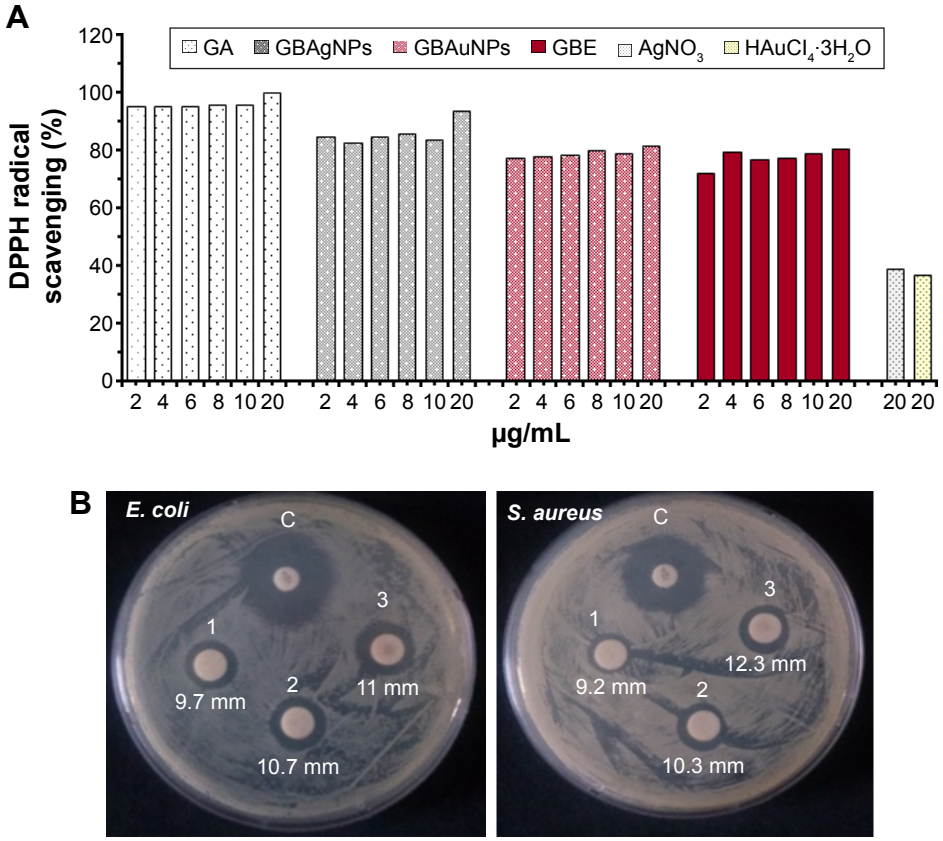

Figure 7 AuNPs and AgNPs synthesized from GBE exhibited free radical scavenging activity.
Notes: (**A**) Comparative DPPH radical scavenging activity of gallic acid, GBAgNPs, GBAuNPs, GBE, and gold and silver salts. GBAgNPs showed the highest free radical scavenging activity (93.8%) compared to GBAuNPs (81.5%) and GBE (81%). AgNPs have antimicrobial activity against Gram-negative (*E. coli*) and Gram-positive (*S. aureus)* bacterial strains. (**B**) Antibacterial activity of GBAgNPs of various concentrations (1, 15 µg/disk; 2, 30 µg/disk and 3, 45 µg/disk) of synthesized GBAgNPs using GBE. Neomycin was used as assay control.
Abbreviations: AgNPs, silver nanoparticles; AuNPs, gold nanoparticles; C, control; DPPH, 2,2-diphenyl-1-picrylhydrazyl; *E. coli*, *Escherichia coli*; GA, gallic acid; GBAgNPs, AgNPs from ginseng berry; GBAuNPs, AuNPs from ginseng berry; GBE, ginseng berry extract; *S. aureus*, *Staphylococcus aureus*.

to the adsorption of existing bioactive compounds of GBE over spherically shaped nanoparticles having a larger surface area. The interaction of plant metabolites with metal ions during nanoparticle formation may result in improved free radical scavenging compounds. In addition, the electrostatic attractions between negatively charged phytochemicals and positively or neutrally charged AgNPs act synergistically to improve the bioactivity of plants.

Effect of GBAuNPs and GBAgNPs on mushroom tyrosinase inhibition

The inhibitory effect of GBE, GBAuNPs, GBAgNPs, and arbutin on the activity of mushroom tyrosinase for the oxidation of L-DOPA was investigated by UV–vis spectrophotometer. Table 2 shows the tyrosinase inhibitor concentration of the compounds leading to 50% activity loss (IC_{50}). GBAgNPs showed the strongest inhibitory activity among the evaluated compounds. GBE and GBAuNPs have similar IC_{50}. Furthermore, arbutin, a typical tyrosinase inhibitor, was found to be less effective on tyrosinase activity compared to the other studied samples. Anti-tyrosinase activity of AuNPs and AgNPs synthesized from GBE could be from flavonoids absorbed by AgNPs and AuNPs, the flavonoids are able to chelate the two copper units from the active site of the tyrosinase enzyme.[37]

Antimicrobial activity of GBAgNPs

Our study showed that the synthesized GBAgNPs had antimicrobial activity against Gram-negative (*E. coli*) and Gram-positive (*S. aureus*) bacterial strains (Figure 7B). Both strains

Table 2 Tyrosinase inhibitory activity using L-DOPA as substrate

Compound	IC_{50}[a] (µg/mL)
GBAgNPs	0.4±0.1
GBAuNPs	6.6±0.3
GBE	7.7±0.6
Arbutin	8.3±0.1

Note: [a]Values are mean ± SD of triplicate measurements.
Abbreviations: GBE, ginseng berry extract; L-DOPA, L-3,4-dihydroxyphenylalanin; GBAgNPs, silver nanoparticles from ginseng berry; GBAuNPs, gold nanoparticles from ginseng berry; IC_{50}, half maximal inhibitory concentration; SD, standard deviation.

were susceptible toward different concentrations of GBAgNPs (1, 15 µg/disk; 2, 30 µg/disk; and 3, 45 µg/disk). The highest zone of inhibition for *E. coli* was 11 mm, and for *S. aureus* it was 12.3 mm treated with 45 µg/disk. Various report suggested that the antimicrobial efficacy of nanoparticles is shape and size dependent; thus, the efficacy of GBAgNPs against bacterial pathogens can be attributed to different shapes and sizes of GBAgNPs synthesized by GBE.[38] Moreover, the various components of GBE attached on the surface of GBAgNPs play a major role in the antimicrobial efficacy.

In vitro cytotoxicity assay of GBAuNPs and GBAgNPs

The development of more effective and biocompatible nanoparticles is incumbent for treating particular diseases as well as maintaining their remediable properties as active drug carriers in cosmetics. AgNPs are strong candidates for possessing a broad spectrum of antimicrobial activities.[39] However, it is important to evaluate their cytotoxic effects on normal cells to ensure their safe use in humans. To assess the potential cytotoxicity of GBAuNPs and GBAgNPs, we selected normal HDF and murine melanoma B16 cell lines and exposed to them with different concentrations of GBAuNPs and GBAgNPs (1–100 µg/mL) for 72 h. Control wells were incubated with fresh culture media, and experiments were repeated in triplicates. For GBAuNPs-treated HDF and B16 cells, there were no visible changes in the cell morphology between the treated cells with 1 µg/mL and control groups at different times (Figure 8A). Treated HDF and B16 cells with AgNPs (10 µg/mL) and AuNPs (10 and 100 µg/mL) could be identified by dark dense clusters as indicated with arrows in Figure 9A. In contrast, no cluster was found in control groups.

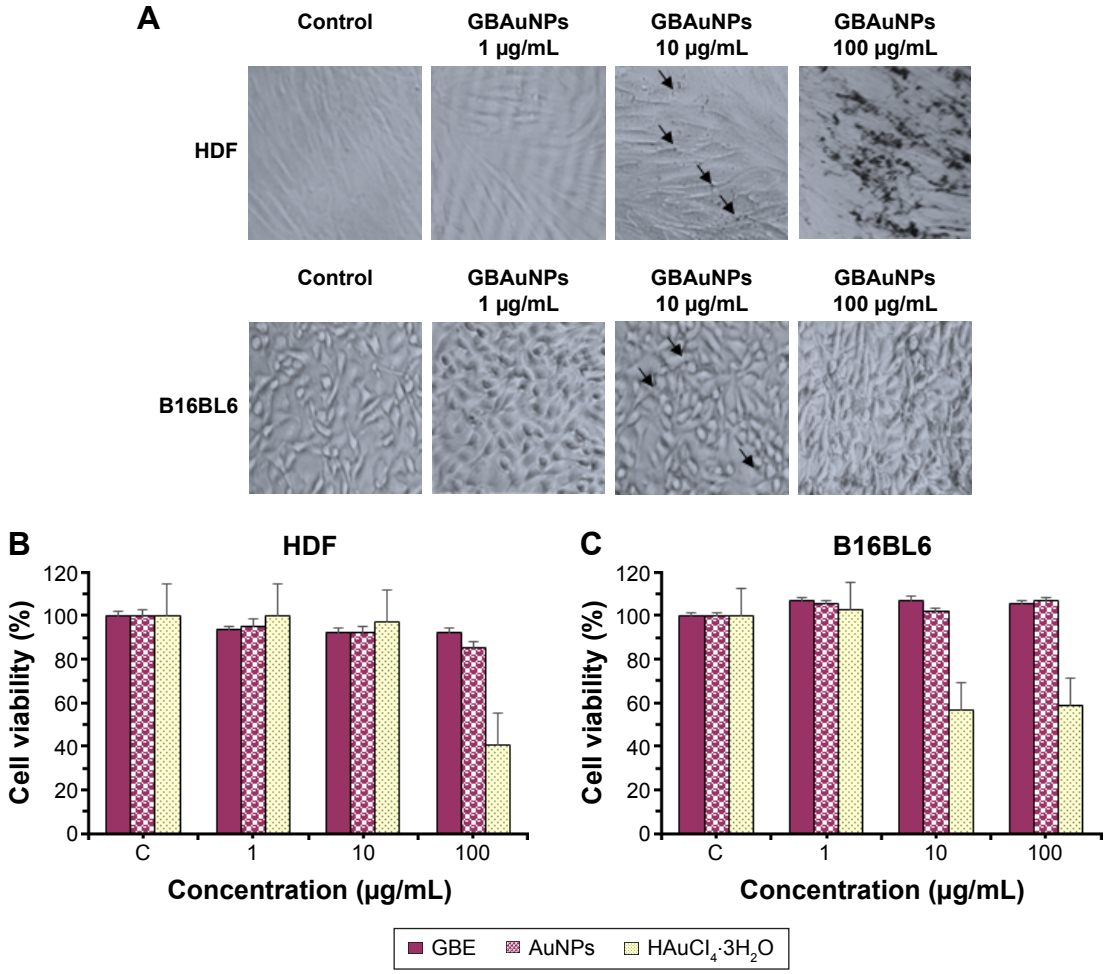

Figure 8 Comparative study of the effect of GBAuNPs, GBE and $HAuCl_4 \cdot 3H_2O$ on cell viability and on the morphology of HDF and B16 cells.
Notes: Optical microscopy images (**A**) of HDF and B16 cell lines (40× magnification) at 72 h after treated with 1–100 µg/mL of GBAuNPs. Treated HDF and B16 cells with AuNPs (10 and 100 µg/mL) could be identified by dark dense clusters which are indicated with arrows; no cluster was found in control groups. Cytotoxicity effect of GBE and GBAuNPs on HDF (**B**) and B16BL6 (**C**) cell lines; GBAuNPs did not exhibit a significant cytotoxic effect on HDF and B16 cells. Cell viability was determined by MTT assay. Data are expressed as a percentage of sample-treated control and presented as mean ± SEM of three separate experiments. B16, murine melanoma B16BL6 cells.
Abbreviations: AuNPs, gold nanoparticles; GBAuNPs, AuNPs from ginseng berry; GBE, ginseng berry extract; HDF, human dermal fibroblast; SEM, standard error of the mean.

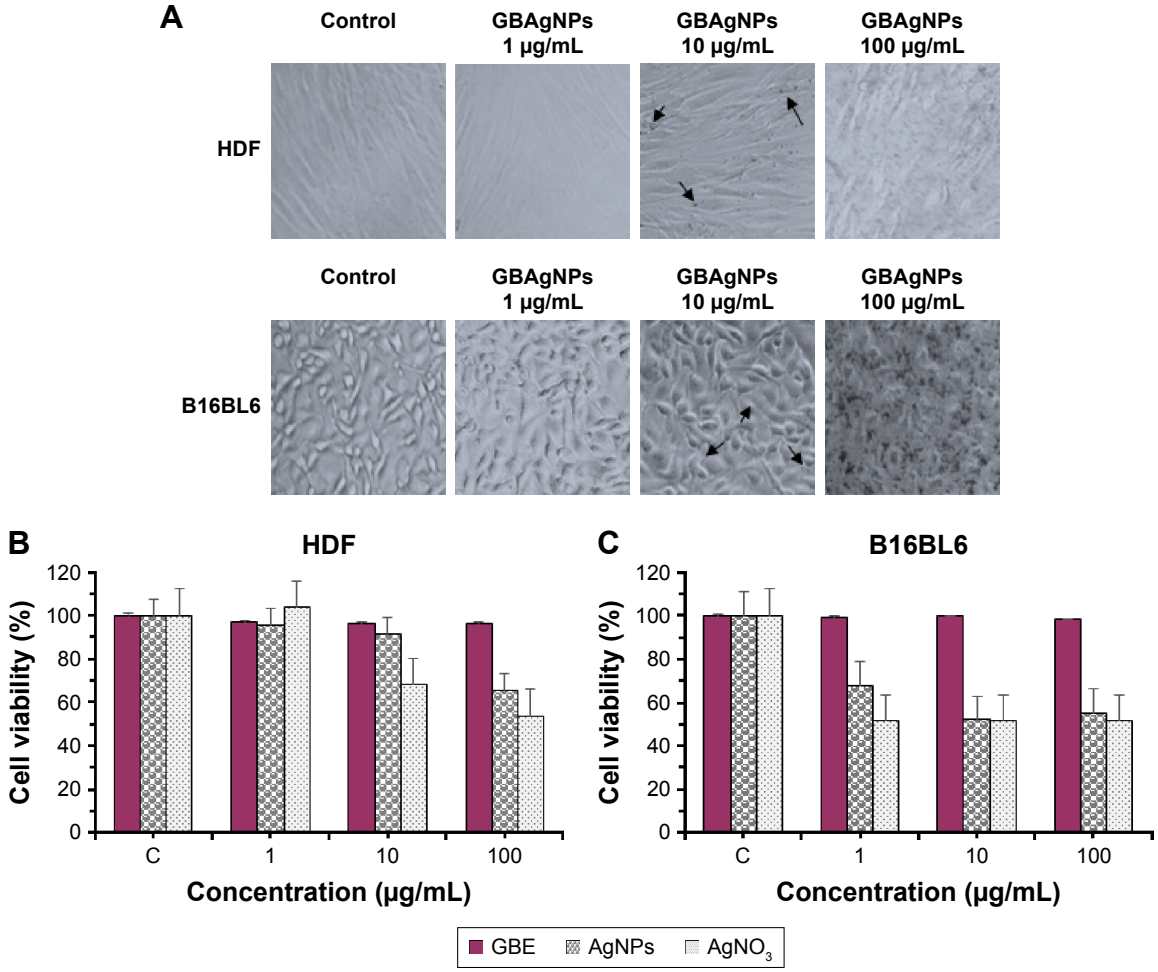

Figure 9 Comparative study of the effect of GBAgNPs, GBE and $AgNO_3$ on cell viability and on the morphology of HDF and B16 cells.
Notes: Optical microscopy images (**A**) of HDF and B16 cell lines (40× magnification) at 72 h after treated with 1–100 µg/mL of GBAgNPs. Treated HDF and B16 cells with silver (10 µg/mL) could be identified by dark dense clusters which are indicated with arrows; no cluster was found in control groups. Cytotoxicity effect of GBE, GBAgNPs, and silver salts on HDF (**B**) and B16 (**C**) cell lines; cell viability decreased with an increase in the concentration of GBAgNPs. Cell viability was determined by MTT assay. Data are expressed as a percentage of sample-treated control and presented as mean ± SEM of three separate experiments.
Abbreviations: B16, murine melanoma B16Bl6 cells; GBAgNPs, silver nanoparticles from ginseng berry; GBE, ginseng berry extract; HDF, human dermal fibroblast; MTT, 3-(4,5-dimethyl-thiazol-2yl)-2, 5-diphenyl tetrazolium bromide; SEM, standard error of the mean.

The quantity of nanoparticles observed corresponded to the concentrations of AuNP and AgNP treatment. Approximately 100 µg/mL of GBAuNP-treated cells had the highest amount of nanoparticle clusters, while cells treated with lower concentration of nanoparticles (1 and 10 µg/mL) had smaller amount of nanoparticle clusters. Previous studies have reported that AgNPs and AuNPs were uptaken by cells via the clathrin-mediated endocytosis pathway.[40,41] This finding suggests that GB-capped AuNPs and AgNPs could be taken up by HDF and B16 cells in a similar manner.

In our study, the cytotoxicity of GBAgNPs and GBAuNPs was evaluated by cell viability assay after 72 h. It was shown that GBAuNPs did not exhibit a significant cytotoxic effect on HDF and B16 cells at any concentrations (1–100 µg/mL; Figure 8B and C). However, cell proliferation of HDF and B16 cell lines was more sensitive to GBAgNPs; cell viability decreased with an increase in the concentration of GBAgNPs (Figure 9B and C). Cells treated with $HAuCl_3 \cdot 3H_2O$ and $AgNO_3$ solutions, which were used as indicator of toxicity (1–100 µg/mL), also demonstrated similar behavior (Figures 8B and C and 9B and C). In short, GBAgNPs were found to be toxic to B16 cells (IC_{50}, 114.8 µg/mL), but comparatively less toxic for HDF cells (IC_{50}, 148.6 µg/mL). Our results also indicated that GBAgNPs synthesized from GBE were less toxic than previously reported biogenic AgNPs and AuNPs.[42,43] Hence, the current investigation suggests that at limited dosage, the GBE-mediated AgNPs can be used as effective skin drug delivery agents with minimum toxicity.

Conclusion

Considering the phytochemical profile and pharmacological efficacies of *P. ginseng* berries in biomedicine, we have

successfully exploited GBE to synthesize AuNPs and AgNPs with functional in vitro biological applications by green chemistry. GBAgNPs showed the highest level of DPPH radical scavenging activity followed by GBE and GBAuNPs. In addition, GBAgNPs possess strong anti-tyrosinase activity compared to GBAuNPs and GBE.

However, the low IC_{50} value of GBAuNps and GBE confirmed that both compounds have higher anti-tyrosinase activity than arbutin. In addition, GBAgNPs exhibited effective antibacterial efficacy against *E. coli* and *S. aureus*. GBAuNPs were nontoxic to HDF and B16 cell lines. However, GBAgNPs were found to be toxic to B16 cells but comparatively less toxic to HDF cells. Thus, the current results suggested that the GB-capped AgNPs could act as potential agents for antibacterial, antioxidant, and anti-tyrosinase activities. Furthermore, GB-capped AuNPs can be used as antioxidant and protective skin agents in cosmetic products, and mediators in drug delivery. Consequently, the study showed the advantages of using nanotechnology and green chemistry to enhance the natural properties of GBs.

Acknowledgments

This research was supported by the Korea Institute of Planning and Evaluation for Technology in Food, Agriculture, Forestry and Fisheries, Republic of Korea (KIPET no: 313038-03-2-SB010) and the Next-Generation BioGreen 21 Program (SSAC, grant#: PJ0120342016), Rural Development Administration, Republic of Korea.

Author contributions

Conceived and designed the experiments: ZEJP, YJK, RM, JM, and RA. Performed the experiments: ZEJP, JM, RA, DW, KHS, and VS. Analyzed the data: ZEJP, JM, RM, RA, and VS. Wrote the manuscript: ZEJP and JM. All authors contributed toward data analysis, drafting and critically revising the paper and agree to be accountable for all aspects of the work.

Disclosure

The authors report no conflicts of interest in this work.

References

1. Thakkar KN, Mhatre SS, Parikh RY. Biological synthesis of metallic nanoparticles. *Nanomed Nanotech Biol Med*. 2010;6(2):257–262.
2. Yun TK. Brief introduction of *Panax ginseng* CA Meyer. *J Korean Med Sci*. 2001;16(suppl):S3–S5.
3. Attele AS, Wu JA, Yuan CS. Ginseng pharmacology: multiple constituents and multiple actions. *Biochem Pharmacol*. 1999;58(11):1685–1693.
4. Jin Y, Kim YJ, Jeon JN, et al. Effect of white, red and black ginseng on physicochemical properties and ginsenosides. *Plant Foods Hum Nutr*. 2015;70(2):141–145.
5. Dey L, Xie J, Wang A, Wu J, Maleckar S, Yuan CS. Anti-hyperglycemic effects of ginseng: comparison between root and berry. *J Phytomed*. 2003;10(6–7):600–605.
6. Joo KM, Lee JH, Jeon HY, et al. Pharmacokinetic study of ginsenoside Re with pure ginsenoside Re and ginseng berry extracts in mouse using ultra performance liquid chromatography/mass spectrometric method. *J Pharm Biomed Anal*. 2010;51(1):278–283.
7. Kim J, Cho SY, Kim SH, et al. Ginseng berry and its biological effects as a natural phytochemical. *Nat Prod Chem Res*. 2016;4:209.
8. Zhang W, Cho SY, Xiang G, Min KJ, Yu Q, Jin JO. Ginseng berry extract promotes maturation of mouse dendritic cells. *PLoS One*. 2015;10(6):e0130926.
9. Lee YR, Noh EM, Jeong EY, Yun SK, Jeong YJ, Kim JH. Cordycepin inhibits UVB-induced matrix metalloproteinase expression by suppressing the NF-κB pathway in human dermal fibroblasts. *Exp Mol Med*. 2009;41(8):548–554.
10. Yeom M, Center R, Lee J, et al. The anti-aging effects of Korean ginseng berry in the skin. *Korean J Pharmacogn*. 2010;41(1):26–30.
11. Jeon JM, Choi SK, Kim YJ, Jang SJ, Cheon JW, Lee HS. Antioxidant and antiaging effect of ginseng berry extract fermented by lactic acid bacteria. *J Soc Cosmet Sci Korea*. 2011;37:75–81.
12. Kim J, Cho SY, Kim SH, et al. Effects of Korean ginseng berry on skin antipigmentation and antiaging via FoxO3a activation. *J Ginseng Res*. 2016 In Press.
13. Rai M, Yadav A, Gade A. Silver nanoparticles as a new generation of antimicrobials. *Biotechnol Adv*. 2009;27(1):76–83.
14. Blumenkrantz N, Asboe-Hansen G. New method for quantitative determination of uronic acids. *Anal Biochem*. 1973;54(2):484–489.
15. Abbai R, Mathiyalagan R, Markus J, et al. Green synthesis of multifunctional silver and gold nanoparticles from the oriental herbal adaptogen: Siberian ginseng. *Int J Nanomedicine*. 2016;11:3131.
16. Kalaiselvi M, Subbaiya R, Selvam M. Synthesis and characterization of silver nanoparticles from leaf extract of *Parthenium hysterophorus* and its anti-bacterial and antioxidant activity. *Int J Curr Microbiol App Sci*. 2013;2:220–222.
17. Tada T, Ohnishi K, Komiya T, Imai K. Synthetic search for cosmetic ingredients: preparations, tyrosinase inhibitory and antioxidant activities of caffeic amides. *J Oleo Sci*. 2002;51:19–27.
18. Singh P, Kim YJ, Singh H, et al. Biosynthesis, characterization, and antimicrobial applications of silver nanoparticles. *Int J Nanomedicine*. 2015;10:2567–2577.
19. Lee J, Jung E, Lee J, et al. *Panax ginseng* induces human type I collagen synthesis through activation of Smad signaling. *J Ethnopharmacol*. 2007;109(1):29–34.
20. Yoo DS, Rho HS, Lee YG, et al. Ginsenoside F1 modulates cellular responses of skin melanoma cells. *J Ginseng Res*. 2011;35:86–91.
21. Raveendran P, Fu J, Wallen SL. Completely "green" synthesis and stabilization of metal nanoparticles. *J Am Chem Soc*. 2003;125(46):13940–13941.
22. Lee SY, Kim YK, Park NI, Kim CS, Lee CY, Park SU. Chemical constituents and biological activities of the berry of *Panax ginseng*. *J Med Plants Res*. 2010;4:349–353.
23. Park KM, Kim YS, Jeong TC, et al. Nitric oxide is involved in the immunomodulating activities of acidic polysaccharide from *Panax ginseng*. *Planta Med*. 2001;67(2):122–126.
24. Kim HJ, Kim MH, Byon YY, Park JW, Jee Y, Joo HG. Radioprotective effects of an acidic polysaccharide of *Panax ginseng* on bone marrow cells. *J Vet Sci*. 2007;8(1):39–44.
25. Mountrichas G, Pispas S, Kamitsos EI. Effect of temperature on the direct synthesis of gold nanoparticles mediated by poly (dimethylaminoethyl methacrylate) homopolymer. *J Phys Chem C*. 2014;118:22754–22759.
26. Begum NA, Mondal S, Basu S, Laskar RA, Mandal D. Biogenic synthesis of Au and Ag nanoparticles using aqueous solutions of Black Tea leaf extracts. *Colloids Surf B*. 2009;71(1):113–118.
27. Ahmad A, Syed F, Shah A, et al. Silver and gold nanoparticles from *Sargentodoxa cuneata*: synthesis, characterization and antileishmanial activity. *RSC Adv*. 2015;5:73793–73806.

28. Link S, El-Sayed MA. Size and temperature dependence of the plasmon absorption of colloidal gold nanoparticles. *J Phys Chem B*. 1999;103:4212–4217.
29. Tran HV, Dai Tran L, Ba CT, et al. Synthesis, characterization, antibacterial and antiproliferative activities of monodisperse chitosan-based silver nanoparticles. *Colloids Surf A Physicochem Eng Asp*. 2010; 360:32–40.
30. Wang C, Singh P, Kim YJ, et al. Characterization and antimicrobial application of biosynthesized gold and silver nanoparticles by using *Microbacterium resistens*. *Artif Cells Nanomed Biotechnol*. 2015;44(7):1714–1721.
31. Singh P, Kim YJ, Wang C, Mathiyalagan R, Farh MEA, Yang DC. Biogenic silver and gold nanoparticles synthesized using red ginseng root extract, and their applications. *Artif Cells Nanomed Biotechnol*. 2015;44(3):780–791.
32. Personick ML, Mirkin CA. Making sense of the mayhem behind shape control in the synthesis of gold nanoparticles. *J Am Chem Soc*. 2013; 135(49):18238–18247.
33. Akhter KF, Mumin MA, Lui EK, Charpentier PA. Microfluidic synthesis of ginseng polysaccharide nanoparticles for immunostimulating action on macrophage cell lines. *ACS Biomater Sci Eng*. 2016;2:96–103.
34. Stuart B. *Infrared spectroscopy*. *Kirk-Othmer Encyclopedia of Chemical*. *Technology*. Hoboken: Wiley Online Library; 2005.
35. Song JY, Jang H-K, Kim BS. Biological synthesis of gold nanoparticles using *Magnolia kobus* and *Diopyros kaki* leaf extracts. *Process Biochem*. 2009;44:1133–1138.
36. Otari S, Patil R, Nadaf N, Ghosh S, Pawar S. Green biosynthesis of silver nanoparticles from an actinobacteria *Rhodococcus* sp. *Mater Lett*. 2012;72:92–94.
37. Kim YJ, Uyama H. Tyrosinase inhibitors from natural and synthetic sources: structure, inhibition mechanism and perspective for the future. *Cell Mol Life Sci*. 2005;62(15):1707–1723.
38. Salunke BK, Shin J, Sawant SS, Alkotaini B, Lee S, Kim BS. Rapid biological synthesis of silver nanoparticles using *Kalopanax pictus* plant extract and their antimicrobial activity. *Korean J Chem Eng*. 2014;31:2035–2040.
39. Paul B, Bhuyan B, Purkayastha DD, Dhar SS. Photocatalytic and antibacterial activities of gold and silver nanoparticles synthesized using biomass of *Parkia roxburghii* leaf. *J Photochem Photobiol B*. 2016;154:1–7.
40. Li JJ, Zou L, Hartono D, Ong CN, Bay BH, Lanry Yung LY. Gold nanoparticles induce oxidative damage in lung fibroblasts in vitro. *Adv Mater*. 2008;20:138–142.
41. Chithrani BD, Ghazani AA, Chan WC. Determining the size and shape dependence of gold nanoparticle uptake into mammalian cells. *Nano Lett*. 2006;6(4):662–668.
42. Manivasagan P, Alam MS, Kang K-H, Kwak M, Kim SK. Extracellular synthesis of gold bionanoparticles by *Nocardiopsis* sp. and evaluation of its antimicrobial, antioxidant and cytotoxic activities. *Bioprocess Biosyst Eng*. 2015;38(6):1167–1177.
43. Kanipandian N, Kannan S, Ramesh R, Subramanian P, Thirumurugan R. Characterization, antioxidant and cytotoxicity evaluation of green synthesized silver nanoparticles using *Cleistanthus collinus* extract as surface modifier. *Mater Res Bull*. 2014;49:494–502.